

Open and hidden strangeness with kaons and φ -mesons in Bjorken energy density approach for central A+A collisions from SPS to LHC

O. Shaposhnikova^{a,b1}, A. Marova^{b2}, G. Feofilov^{b3}

O.M. Шапошникова^{a,b1}, А.А. Марова^{b,22}, Г.А. Феофилов^{b,23}

^a Moscow State University

^a Московский государственный университет

^b Saint-Petersburg State University

^b Санкт-Петербургский государственный университет, Россия, 199034,
Санкт-Петербург, Университетская наб. 7/9

С целью сравнения вкладов в плотность энергии Бьоркена мы используем имеющиеся данные о значениях $\langle dN/dy \rangle$ и $\langle p_T \rangle$ для адронов, в том числе для $\pi^+ + \pi^-$, $K^+ + K^-$, $p + \bar{p}$, $K^*(892)^0$ и φ -мезонов, зарегистрированных в области нулевых быстрот ($|y| < 0.5$) в центральных 0-5% столкновениях Au-Au, Pb-Pb и Xe+Xe в широком диапазоне энергий. Частицы типа странно-нейтрального φ -мезона (система $s\bar{s}$ кварков) и K-мезона (содержащего одиночный s-кварк) представляют особый интерес, поскольку они могут иметь разные механизмы рождения и чувствительности к свойствам кварк-глюонной плазмы.

We use the available data on $\langle dN/dy \rangle$ and $\langle p_T \rangle$ for the identified hadrons including $\pi^+ + \pi^-$, $K^+ + K^-$, $p + \bar{p}$, $K^*(892)^0$ and φ -mesons, registered at midrapidity ($|y| < 0.5$) in central 0-5% Au-Au, Pb-Pb and Xe+Xe collisions in a broad range of energies in order to compare the relative contributions to the Bjorken energy density. Particles, like strangeness-neutral φ -meson (a system of $s\bar{s}$ quarks) and K-meson (containing single s-quark), are of specific interest because they might have different production mechanisms and differ in sensitivity to the properties of the QGP-medium formed in relativistic heavy-ion collisions.

PACS: 44.25.+f; 44.90.+c

Introduction

According to the prediction in [1] by J.Rafelski and B. Müller, the formation of quark-gluon plasma (QGP) in relativistic nucleus-nucleus collisions would result in an increased yield of particles containing strange quarks, if compared to the proton-proton case. The formation of s and \bar{s} quarks can

¹E-mail: shaposhnikova.om23@physics.msu.ru

²E-mail: st097602@student.spbu.ru

³E-mail: g.feofilov@spbu.ru

¹E-mail: shaposhnikova.om23@physics.msu.ru(русский вариант)

²E-mail: st097602@student.spbu.ru(русский вариант)

³E-mail: g.feofilov@spbu.ru(русский вариант)

be increased in the QGP due to the multiple perturbative gluon-gluon interactions of the $gg \rightarrow s\bar{s}$ type, as well as in the processes $u\bar{u}, d\bar{d} \rightarrow s + \bar{s}$. Non perturbative processes could dominate the production of strange hadrons at low p_T where the phenomenological models with fragmentation of quark-gluon strings could be applied with the account of some collectivity effects.

The decisive role of open strangeness as a characteristic feature and signal of the formation of quark-gluon plasma was confirmed, in particular, in experiments such as NA57 [2] and NA51/SHINE [3–5] at SPS at CERN and in STAR [6], [7] at the collider RHIC at BNL. An increased yield of strangeness was also found later by ALICE at the LHC in the high multiplicity events collisions of small systems (pp and $p + Pb$) [8].

The short-lived φ -meson is of particular interest since it is the lightest of the vector mesons with the hidden flavor. The quark composition of φ -meson can be thought of as a mixture of $s\bar{s}$, $u\bar{u}$ and $d\bar{d}$ states, but it is considered to be very close to the pure $s\bar{s}$ state.

The OZI rule [9] strongly influences the rate of birth and decay of φ -meson, suppressing its decay to three pions and causing it to predominantly decay in a pair of $K^+ + K^-$ mesons.

Additionally, [10] suggests that the absence of OZI suppression can lead to a significant increase in the production of φ -mesons during the formation of the QGP. You can find a review of measurements of φ -meson yields in [11].

We present below a comparative analysis and discuss the $\sqrt{s_{NN}}$ dependences of the contributions by the identified particles like φ -mesons and $K^*(892)^0$ resonances and, as well as by $K^+ + K^-$, $\pi^+ + \pi^-$ and $p + \bar{p}$ hadrons to the Bjorken energy density related to the interaction region in the most central (0-5%) nucleus-nucleus collisions.

1. Bjorken energy density

Following [12], the Bjorken energy density ϵ (1) is determined at midrapidity through the mean transverse energy dE_{\perp}/dy by the particles formed in the volume of a cylinder with a cross-sectional area S_{\perp} determined by the overlap between colliding nuclei and the length corresponding to the characteristic particle formation time τ :

$$\epsilon = \frac{dE_{\perp}}{dy} \cdot \frac{1}{S_{\perp}\tau} \quad (1)$$

With the transverse mass of an identified hadron $\langle m_{\perp} \rangle = \sqrt{m^2 + p_T^2}$, one can approximate the mean transverse-energy rapidity density, relevant to the given centrality class of collisions, with a sum (2) of contributions by different hadrons. In our estimates of components of $\frac{dE_{\perp}}{dy}$, we used the available published data with the experimental values of $\langle dN/dy \rangle$ and $\langle p_T \rangle$ obtained in [13–18]. This includes also resonances $K^*(892)^0$ and φ -mesons registered in the central rapidity region in a wide energy range of nucleus-nucleus collisions (from the SPS to the LHC).

The majority of Bjorken energy density estimates are widely using the quantity of $\epsilon \cdot \tau$ (3) with the particle formation time $\tau = 1$ fm/c. Our study also follows this approach.

We have to note also that the Bjorken energy density approach may not be entirely accurate at the energies below RHIC, because the formation time (τ) should be larger than the time of passage of the colliding nuclei through each other [19].

$$\frac{dE_{\perp}}{dy} = \frac{3}{2} \langle m_{\perp} \rangle \frac{dN}{dy}_{\pi^{\pm}} + 2 \langle m_{\perp} \rangle \frac{dN}{dy}_{K^{\pm}, p, \bar{p}} + \langle m_{\perp} \rangle \frac{dN}{dy}_{K^{*}(892)^0} + \langle m_{\perp} \rangle \frac{dN}{dy}_{\varphi} \quad (2)$$

$$\epsilon \cdot \tau = \frac{dE_{\perp}}{dy} \cdot \frac{1}{S_{\perp}} \quad (3)$$

The quantity of $\epsilon \cdot \tau$ (3) still contains another parameter - the transverse area S_{\perp} , one cannot measure it directly. The usual methods to define it are based on the Glauber Monte Carlo (GMC) approach combined with the multiplicity distribution analysis where the estimated mean number of participating nucleons (N_{part}) is considered to be in the relation to the transverse area [3, 8].

In our study, instead of the GMC, we assume that the measured particle production is straightforwardly related to the geometry of partially overlapping nuclei.

Calculations, assuming colliding disks of radii $R = 6.87$ fm [6] for Au–Au collisions (or $R = 7.17$ fm [17] for Pb–Pb collisions), show that in both cases the dominant events selected in a given central 0–5% class will have a noticeable shift of the average impact parameter $\langle b \rangle$ from 0. The following values could be obtained for the class 0–5% Au–Au collisions: $\langle b \rangle = 2.18$ fm, and for 0–5% Pb–Pb collisions – $\langle b \rangle = 2.26$ fm. (In both cases we estimate the accuracy of $\langle b \rangle$ value to be ~ 0.2 fm). Naturally, this will lead to a smaller value of the overlap area if compared to $\langle b \rangle = 0$. The GMC calculations for central Au–Au collisions that gave also similar results for $\langle b \rangle \sim 2.2, 2.39, 2.21$ fm at three RHIC energies, see [6]. Therefore, in our approach we use the following corrected value of the mean initial transverse area S_{\perp} for the given classes of central events 0–5% of Au–Au and Pb–Pb collisions: 118.5 ± 2.9 fm² and 129.5 ± 2.2 fm². Naturally, this results in about 20% higher values of $\epsilon \cdot \tau$ then in the usually applied GMC. (We may also argue that our straightforward approach should give a smaller systematic bias on the final results).

In case of collisions of the deformed Xe nuclei ($\beta = 0.18 \pm 0.02$) at 5.44 TeV, we used the efficient value $S_{eff\perp}$. We obtained it after the normalization of the relevant values of $\epsilon \cdot \tau$ on the data for pions extrapolated to the energy $\sqrt{s_{NN}} = 5.44$ TeV. This gives for the overlap area of for 0–5% centrality of Xe–Xe collisions the value $S_{eff\perp} = 70.1 \pm 15.6$ fm², that is used further to calculate the contributions to $\epsilon \cdot \tau$ by $K^+ + K^-$, $p + \bar{p}$, $K^{*}(892)^0$ and φ -mesons.

Results

We show in Fig. 1 the results of energy dependence of fractions of $\epsilon \cdot \tau$ as defined in (4) and obtained in our study for the identified hadrons including $\pi^+ + \pi^-$, $K^+ + K^-$, $p + \bar{p}$, $K^*(892)^0$ and φ -mesons. The identified hadrons were measured at midrapidity in central 0-5% Au-Au, Pb-Pb and Xe+Xe collisions in a broad range of collision energies.

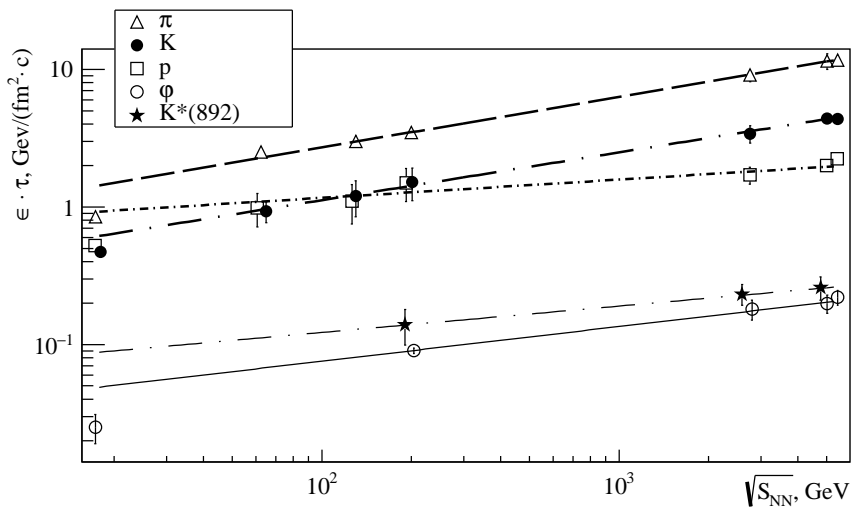


Fig. 1. Values of Bjorken $\epsilon \cdot \tau$ with $\tau = 1 \text{ fm}/c$ in 0 – 5% Au-Au, Pb-Pb and Xe-Xe collisions as a function of $(\sqrt{s_{NN}})$ for identified hadrons (including $\pi^+ + \pi^-$, $K^+ + K^-$, $p + \bar{p}$, $K^*(892)^0$ and φ -meson). Estimates were done using published data on $\langle p_t \rangle$ and $\langle dn/dy \rangle$ measured in [13–18] at midrapidity ($(|y| < 0.5)$, except data at 17.3 GeV, where $(|y| < 0.6)$). Lines – are the results of power-law fits (4). We show only statistical uncertainties. We estimate total systematic uncertainties to be $\leq 10\%$ for Au-Au and Pb-Pb data and $\leq 25\%$ in case of Xe-Xe.

Power-law fits (4) were performed for $\epsilon \cdot \tau$ vs. $\sqrt{s_{NN}}$ data in the region $\sqrt{s_{NN}}$ of 200 GeV – 5.2 TeV. (We note that we take in (4) the quantity s as dimensionless s/s_0 , where $s_0 = 1 \text{ GeV}^2$). One may find the fit parameter values in Table 1.

$$\epsilon \cdot \tau = Q \cdot (s_{NN})^n \quad (4)$$

We observe in Fig.1:

- in case of pions, the s -dependence of $\epsilon \cdot \tau$ is growing faster ($s^{0.184 \pm 0.015}$) then the power-law behaviour in case of the charged particle multiplicities in AA collisions well described by the function $s^{0.155}$ [20];
- for pions, kaons and protons, the s -dependences of $\epsilon \cdot \tau$ demonstrate different behavior from one to another. This is also true for φ -mesons ($s^{0.126 \pm 0.020}$) in comparison to K -mesons ($s^{0.17 \pm 0.03}$);

- the s -dependences of $\epsilon \cdot \tau$ for two resonances – φ -mesons and $K^*(892)^0$, are remarkably similar in the whole energy range (see Fig.1 and Table 1);
- one may note here that the masses of resonances – φ -mesons and $K^*(892)^0$ – (1020 MeV and 892 MeV) are rather close to each other, thus we have a similar behaviour of $\epsilon \cdot \tau$ with energy. However, the mass of proton is even closer to the mass of φ -meson, while the contribution to the s -dependence of $\epsilon \cdot \tau$ by protons is noticeably higher than for φ -mesons or $K^*(892)^0$.

Table 1. Parameters of power-law $Q \cdot (s)^n$ approximations for values of $\epsilon \cdot \tau$ vs. \sqrt{s} for $(\pi^+ + \pi^-)$, $(K^+ + K^-)$, $(p + \bar{p})$, $K^*(892)^0$ and φ -mesons.

	n	Q	χ^2/NDF
π	0.184 ± 0.015	0.50 ± 0.09	0.013/2
K	0.17 ± 0.03	0.23 ± 0.11	0.14/2
p	0.07 ± 0.03	0.6 ± 0.3	0.6/2
$K^*(892)^0$	0.10 ± 0.05	0.05 ± 0.04	0.001/1
φ	0.126 ± 0.020	0.024 ± 0.006	0.05/1

Table 2. Parameters of linear approximations $A + B \cdot (s)$ of ratios of yields of φ -mesons to the relevant yields of $(\pi^+ + \pi^-)$, $(K^+ + K^-)$, $(p + \bar{p})$ and $K^*(892)^0$.

	$(\epsilon \cdot \tau)_\varphi / (\epsilon \cdot \tau)_\pi$	$(\epsilon \cdot \tau)_\varphi / (\epsilon \cdot \tau)_K$	$(\epsilon \cdot \tau)_\varphi / (\epsilon \cdot \tau)_p$	$(\epsilon \cdot \tau)_\varphi / (\epsilon \cdot \tau)_{K^*}$
A	0.026 ± 0.002	0.06 ± 0.01	0.05 ± 0.01	0.7 ± 0.2
$B, 10^{-6}$	-1.5 ± 0.5	-1.6 ± 2.1	9.2 ± 2.7	26.0 ± 55.0
χ^2/ndf	0.8/3	0.4/3	1.8/3	0.11/1

In case of the hidden stranges formation, we see in Fig.1 and with Table 1 data that the Bjorken energy fraction of $\epsilon \cdot \tau$, relevant to φ -mesons, is growing much slower with the collision energy ($s^{0.126 \pm 0.020}$) than the one relevant to pions ($s^{0.184 \pm 0.015}$). We can qualitatively explain this for pions as a result of growth with the collision energy of the mean p_\perp , that contributes to the transverse mass. As to the case of $p + \bar{p}$, we see rather slower growth ($s^{0.17 \pm 0.03}$) with $\sqrt{s_{NN}}$. Taking into account the fact that masses of φ -mesons and $K^*(892)^0$ – (1020 MeV and 892 MeV) are close to the mass of proton (938 MeV) one may assume that the partonic degrees of freedom in QGP are playing a different role in the formation of protons and resonances.

Another observation concerns the ratios of fractions of Bjorken energy density $\epsilon \cdot \tau$ values as a function of collision energies obtained in this work for several identified hadrons. (It is evident that these are the ratios of the relevant transverse energies). In Fig.2 we show the ratios of values of $\epsilon \cdot \tau$ of φ -mesons to the relevant densities for other hadrons: $(\pi^+ + \pi^-)$, $(K^+ + K^-)$, $(p + \bar{p})$ and $K^*(892)^0$.

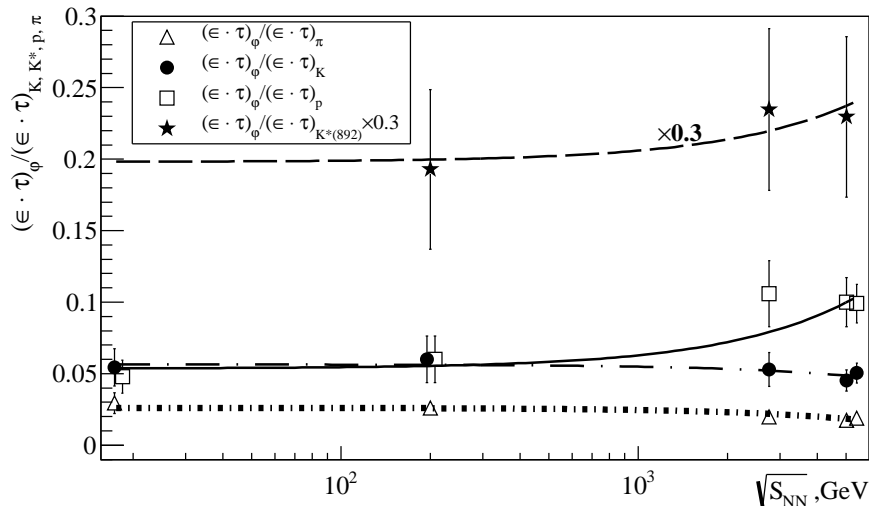


Fig. 2. A) Energy dependence for ratios of values of Bjorken energy densities $(\epsilon \cdot \tau)_\varphi / (\epsilon \cdot \tau)_{(\pi^+ + \pi^-), (K^+ + K^-), (p + \bar{p}, K^*(892)^0)}$. Lines are linear fits $a \cdot s_{NN} + b$ (see Table 2).

In Table 2 we present the parameters of approximation of ratios of particle yields with linear function $A + B \cdot (s)$.

As we see, in the whole region of collision energies under study, these ratios of particle yields $(\epsilon \cdot \tau)_\varphi / ((\epsilon \cdot \tau)_{(\pi^+ + \pi^-), (K^+ + K^-), (p + \bar{p}, K^*(892)^0)})$ are almost flat with $\sqrt{s_{NN}}$ (see Fig.2). A similar flat dependence, but *for the ratios of the yields of φ -mesons to yields of K^-*

was observed earlier in the domain from SPS to RHIC energies (see the compilation of data and analysis in [21]) and at the LHC [22]. Our results of the ratio of the yields $2 \cdot \varphi / (K^+ + K^-) = 0.12 \pm 0.2$ is very near to the mean ratio of yields $\varphi / K^- = 0.15 \pm 0.3$ observed in a wide region of collision energies (see in [21] and [22]).

Among the theoretical models directly focused on medium effects on hidden strangeness production in heavy-ion collisions, we mention just briefly the microscopic Parton-Hadron-String Dynamics (PHSD) transport approach model [21] that was successfully applied to describe the ratios of φ -mesons to yields of K^- observed earlier in the domain from SPS to RHIC energies. PHSD model is a non-equilibrium microscopic transport approach for the description of the dynamics of strongly interacting hadronic and partonic matter. At the region of the LHC energies, the ratio of yields φ -mesons to yields of K^- was described in the statistical hadronization model [23]. One may find also in [22] discussion of a number of different approaches like EPOS3 model calculations with and without a hadronic cascade phase modeled by UrQMD. We may conclude here that the complete understanding of a hidden strangeness production and of the medium produced effects of strangeness still are not quite well understood and this requires the additional studies with new observables.

Conclusions

We calculated the values of mean Bjorken energy density $\epsilon \cdot \tau$ using the available published data with experimental values of $\langle dN/dy \rangle$ and $\langle p_T \rangle$ obtained in ([13] – [18]) for several identified hadrons including strangeness-neutral φ -meson ($s\bar{s}$ quark system), $K^*(892)^0$ and $K^+ + K^-$ mesons (containing single s (or \bar{s})-quark). We obtained estimates for central 0–5% classes of Au–Au, Pb–Pb and Xe–Xe collisions in a wide range of $\sqrt{s_{NN}}$ – up to the highest at the LHC. We took also into account in our calculations of $\epsilon \cdot \tau$ for all colliding systems the fact that in any of central 0–5% class the mean impact parameter value is shifted from 0 to the value of $\sim 2.3 \pm 0.2$ fm. Therefore, we corrected accordingly the transverse area of the interaction region S_{\perp} for central 0–5% classes for all colliding systems used in this analysis.

We observe different dependencies on the collision energy for the fractions of the Bjorken energy density $\epsilon \cdot \tau$. We found that the one relevant to $(\pi^+ + \pi^-)$ grows with s faster ($s^{0.184 \pm 0.015}$) then in case of multiplicity ($s^{0.157}$) [20]. This could be explained by the contribution from the well known growth in AA collisions of the $\langle p_T \rangle$ value for pions with $\sqrt{s_{NN}}$. At the same time, the results for $(p + \bar{p})$ demonstrate the slowest dependence on the energy of collisions: ($s^{0.07 \pm 0.3}$).

We observe also that the ratios of the Bjorken energy fractions, relevant to the identified hadrons - $(\epsilon \cdot \tau)_{\varphi} / ((\epsilon \cdot \tau)_{(\pi^+ + \pi^-), (K^+ + K^-), K^*(892)^0})$, in all cases, are practically not depending on the collision energy. This behavior looks similar to the one previously observed in *the ratios of yields* of φ -mesons to K^- mesons.

It is in our plans to include in these studies of Bjorken energy densities the additional available data of λ hyperons, as well as of the particles containing two or three strange quarks, to compare with the hidden strangeness production in relativistic heavy-ion collisions.

Acknowledgement: Supported by Saint Petersburg State University, project ID: 94031112.

Authors are grateful to Vladimir Kovalenko for useful discussions.

REFERENCES

1. *Rafelski J., Müller B.* Strangeness Production in the Quark-Gluon Plasma // Phys. Rev. Lett. 1982. Apr. V. 48. P. 1066–1069. URL: <https://link.aps.org/doi/10.1103/PhysRevLett.48.1066>.
2. *Antinori F., Bacon P., A Badalà et al. N.C.* Enhancement of hyperon production at central rapidity in 158 A GeV/c PbPb collisions // Journal of Physics G: Nuclear and Particle Physics. 2006. feb. V. 32, no. 4. P. 427. URL: <https://dx.doi.org/10.1088/0954-3899/32/4/003>.

3. *Laszlo A. et al.* [NA61 Collaboration] NA61/Shine at the CERN SPS. 2007. arXiv:0709.1867 [nucl-ex].
4. *Balkova, Yuliia.* Strangeness production in the NA61/SHINE experiment at the CERN SPS energy range // EPJ Web Conf. 2022. V. 271. P. 02013. URL: <https://doi.org/10.1051/epjconf/202227102013>.
5. *Aduszkiewicz A. et al.* [NA61 Collaboration] Recent results from NA61/SHINE // Nuclear Physics A. 2017. V. 967. P. 35–42. The 26th International Conference on Ultra-relativistic Nucleus-Nucleus Collisions: Quark Matter 2017 URL: <https://www.sciencedirect.com/science/article/pii/S0375947417301197>.
6. *Caines H. et al.* [STAR Collaboration] An update from STAR at RHIC using strangeness to probe relativistic heavy ion collisions // Journal of Physics G: Nuclear and Particle Physics. 2003. dec. V. 30, no. 1. P. S61. URL: <https://dx.doi.org/10.1088/0954-3899/30/1/005>.
7. *Shi S., (for the STAR collaboration).* Strangeness in STAR experiment at RHIC // Journal of Physics: Conference Series. 2017. jan. V. 779, no. 1. P. 012008. URL: <https://dx.doi.org/10.1088/1742-6596/779/1/012008>.
8. *J. Adam, D. Adamová, M. M. Aggarwal et al., . et al.* [ALICE Collaboration] Enhanced production of multi-strange hadrons in high-multiplicity proton–proton collisions // Nature Physics. 2017. V. 13. P. 535–539. URL: <https://doi.org/10.1038/nphys4111>.
9. *Okubo S.* Consequences of quark-line (Okubo-Zweig-Iizuka) rule // Phys. Rev. D. 1977. Oct. V. 16. P. 2336–2352. URL: <https://link.aps.org/doi/10.1103/PhysRevD.16.2336>.
10. *Shor A.* φ -Meson Production as a Probe of the Quark-Gluon Plasma // Phys. Rev. Lett. 1985. Mar. V. 54. P. 1122–1125. URL: <https://link.aps.org/doi/10.1103/PhysRevLett.54.1122>.
11. *Md. Nasim, Vipul Bairathi, Mukesh Kumar Sharma, Bedangadas Mohanty and Anju Bhasin.* A Review on phi-Meson Production in Heavy-Ion Collision Meson Production in Heavy-Ion Collision // Advances in High Energy Physics. 2015. V. 2015. P. 1–16. URL: <https://doi.org/10.1155/2015/197930>.
12. *Bjorken J.D.* Highly relativistic nucleus-nucleus collisions: The central rapidity region // Phys. Rev. D. 1983. Jan. V. 27. P. 140–151. URL: <https://link.aps.org/doi/10.1103/PhysRevD.27.140>.
13. *Alt C. et al.* [NA49 Collaboration] Energy dependence of ϕ meson production in central Pb + Pb collisions at $\sqrt{s_{NN}} = 6$ to 17 GeV // Phys. Rev. C. 2008. Oct. V. 78. P. 044907. URL: <https://link.aps.org/doi/10.1103/PhysRevC.78.044907>.

14. *Adcox K. et al.* [PHENIX Collaboration] Measurement of the Midrapidity Transverse Energy Distribution from $\sqrt{s_{NN}} = 130\text{GeV}$ $Au + Au$ Collisions at RHIC // *Phys. Rev. Lett.* 2001. Jul. V. 87. P. 052301. URL: <https://link.aps.org/doi/10.1103/PhysRevLett.87.052301>.
15. *Abelev B. et al.* [ALICE Collaboration] Centrality dependence of π , K , and p production in Pb-Pb collisions at $\sqrt{s_{NN}} = 2.76\text{TeV}$ // *Phys. Rev. C.* 2013. Oct. V. 88. P. 044910. URL: <https://link.aps.org/doi/10.1103/PhysRevC.88.044910>.
16. *Acharya S. et al.* [ALICE Collaboration] System-size dependence of the charged-particle pseudorapidity density at $s_{NN}=5.02\text{TeV}$ for pp, pPb, and PbPb collisions // *Physics Letters B.* 2023. V. 845. P. 137730. URL: <https://www.sciencedirect.com/science/article/pii/S0370269323000643>.
17. *Adam J. et al.* [ALICE Collaboration] Measurement of transverse energy at midrapidity in Pb-Pb collisions at $\sqrt{s_{NN}} = 2.76\text{TeV}$ // *Phys. Rev. C.* 2016. Sep. V. 94. P. 034903. URL: <https://link.aps.org/doi/10.1103/PhysRevC.94.034903>.
18. *Acharya S. et al.* [ALICE Collaboration] Production of charged pions, kaons, and (anti-)protons in Pb-Pb and inelastic pp collisions at $\sqrt{s_{NN}} = 5.02\text{TeV}$ // *Phys. Rev. C.* 2020. Apr. V. 101. P. 044907. URL: <https://link.aps.org/doi/10.1103/PhysRevC.101.044907>.
19. *Litvinenko A.G.* Some Results Obtained at the Relativistic Heavy Ion Collider // *Physics of Particles and Nuclei.* 2007. V. 38. P. 204–231. URL: <https://link.springer.com/article/10.1134/S1063779607020037>.
20. *Adam J. et al.* [ALICE Collaboration] Centrality Dependence of the Charged-Particle Multiplicity Density at Midrapidity in Pb-Pb Collisions at $\sqrt{s_{NN}} = 5.02\text{TeV}$ // *Phys. Rev. Lett.* 2016. Jun. V. 116. P. 222302. URL: <https://link.aps.org/doi/10.1103/PhysRevLett.116.222302>.
21. *Song, Taesoo., Aichelin, Joerg., Bratkovskaya, Elena.* In-medium effects on hidden strangeness production in heavy-ion collisions // *EPJ Web Conf.* 2023. V. 276. P. 03001. URL: <https://doi.org/10.1051/epjconf/202327603001>.
22. *Acharya S. et al.* [ALICE Collaboration Collaboration] Production of $K^*(892)^0$ and $\phi(1020)$ in pp and Pb–Pb collisions at $\sqrt{s_{NN}} = 5.02\text{TeV}$ // *Phys. Rev. C.* 2022. Sep. V. 106. P. 034907. URL: <https://link.aps.org/doi/10.1103/PhysRevC.106.034907>.
23. *Stachel J., Andronic A., Braun-Munzinger P., Redlich K.* Confronting LHC data with the statistical hadronization model // *Journal of Physics: Conference Series.* 2014. may. V. 509, no. 1. P. 012019. URL: <https://dx.doi.org/10.1088/1742-6596/509/1/012019>.